Title	Seasonal changes in mesozooplankton swimmers collected by sediment trap moored at a single station on the Northwind Abyssal Plain in the western Arctic Ocean
Author(s)	Matsuno, Kohei; Yamaguchi, Atsushi; Fujiwara, Amane; Onodera, Jonaotaro; Watanabe, E.; Imai, Ichiro; Chiba, Sanae; Harada, Naomi; Kikuchi, Takashi
Citation	Journal of Plankton Research, 36(2), 490-502. https://doi.org/10.1093/plankt/fbt092
Issue Date	2014-03
Doc URL	http://hdl.handle.net/2115/57993
Rights	This is a pre-copy-editing, author-produced PDF of an article accepted for publication in Journal of Plankton Research following peer review. The definitive publisher-authenticated version J. Plankton Res. (March/April 2014) 36 (2): 490-502. is available online at: http://plankt.oxfordjournals.org/content/36/2/490.full
Type	article (author version)
File Information	72)Matsuno-2014.pdf

1 Seasonal changes in mesozooplankton swimmers collected by sediment trap moored at a single

2 station of Northwind Abyssal Plain in the western Arctic Ocean

3 KOHEI MATSUNO[1]*, ATSUSHI YAMAGUCHI[2], AMANE FUJIWARA[1], JONAOTARO

4 ONODERA[3], EIJI WATANABE[3], ICHIRO IMAI[2], SANAE CHIBA[3], NAOMI HARADA[3] AND

5 TAKASHI KIKUCHI[3]

6 [1]ARCTIC ENVIRONMENT RESEARCH CENTER, NATIONAL INSTITUTE OF POLAR

7 RESEARCH, 10-3 MIDORI-CHO, TACHIKAWA, TOKYO 190-8518, JAPAN,

8 [2]LABORATORY OF MARINE BIOLOGY, GRADUATE SCHOOL OF FISHERIES SCIENCES,

9 HOKKAIDO UNIVERSITY, 3-1-1 MINATO-CHO, HAKODATE, HOKKAIDO 041-8611, JAPAN,

10 [3]JAPAN AGENCY FOR MARINE-EARTH SCIENCE AND TECHNOLOGY,

11 NATSUSHIMA-CHO 2-15, YOKOSUKA, KANAGAWA 237-0061, JAPAN

12 * CORRESPONDING AUTHOR: matsuno.kohei@nipr.ac.jp, k.matsuno@fish.hokudai.ac.jp

13 KEYWORDS: copepods; life cycle; Pacific water; sea ice; sediment trap

14 RUNNING HEAD: Seasonal changes of mesozooplankton in Arctic Ocean

Abstract

To examine seasonal changes in mesozooplankton community, analyses were made on the swimmer samples (>1 mm) collected by a sediment trap mooring at 184 m depth of Northwind Abyssal Plain in the western Arctic Ocean during October 2010 to September 2011.   The zooplankton swimmer flux ranged 5−44 ind. m^{-2} day^{-1} and was greater during July to October; copepods were the dominant taxon.   Based on the zooplankton swimmer flux, cluster analysis classified samples into three groups (A, B-1 and B-2).   The occurrence of each group showed clear seasonality; group A was observed during July to October, group B-1 was seen in November to January, and group B-2 was seen during March to June.   The seasonal variability in population structures of four dominant copepod swimmers were clearly different among the species.   Most *Calanus hyperboreus* were C6F throughout the year.   For *Metridia longa* and *Paraeuchaeta glacialis*, C6Fs dominated during January to May, and early copepodid stages increased during June to October.   *Heterorhabdus norvegicus* was dominated by C5 during November to February, and C6F/M during March to May.   Since Pacific copepods (*Neocalanus cristatus*) occurred with significant number during August−September, possible causes are discussed.

INTRODUCTION

After 1990's, a drastic reduction of sea ice cover area has been observed in the Arctic Ocean during summer (July−October).   This reduction is considered to have been caused by an increased flow of warm Pacific Summer Water (PSW) from the Bering Sea Strait into the Arctic Ocean (Shimada *et al.*, 2006; Woodgate *et al.*, 2010).   The Pacific sector of the Arctic Ocean comprises both shallow (Chukchi Sea and East Siberian Sea) and deep (Canada Basin and Mendeleyev Ridge) areas (Fig. 1).   Sea ice reduction in this region has been the greatest in the Arctic Ocean (Shimada *et al.*, 2001, 2006; Stroeve *et al.*, 2007; Comiso *et al.*, 2008; Markus *et al.*, 2009), and this reduction of sea ice is expected to alter the marine ecosystem structure in the Arctic Ocean (Grebmeier *et al.*, 2006; Hunt and Drinkwater, 2007; Grebmeier, 2012).

The zooplankton community in the western Arctic Ocean has been studied based on net

2

samples (Springer *et al.*, 1989; Darnis *et al.*, 2008; Hopcroft *et al.*, 2010; Matsuno *et al.*, 2011, 2012).   However, seasonal sea ice coverage in this area prevents collection of net samples in winter, and most of the studies were conducted only in summer.   To evaluate seasonal changes in zooplankton community, analysis on zooplankton swimmers (Knauer *et al.*, 1979) collected by moored sediment trap is a powerful tool (cf. Forbes *et al.*, 1992).   According to Knauer *et al.* 1979, swimmer is defined that zooplankton actively swam into the trap and was killed by the preservation fluid filled with the cups.   Because of their importance, seasonal changes in swimmer community collected by sediment trap have been studied in several areas of the Arctic Ocean, especially in the Beaufort Sea (Forbes *et al.*, 1992; Ota *et al.*, 2008; Makabe *et al.*, 2010).   According to Makabe *et al.* (2010), seasonal changes in Arctic swimmer community are related to the sea ice concentration, temperature and salinity.   This is partly because large copepods migrate to surface when the sea ice melts (Conover and Huntley, 1991), graze on phytoplankton in the ice-edge bloom (Springer and McRoy, 1993), and then reproduce.   The reproduction seasons of dominant copepods vary with species and areas within the Arctic Ocean (Falk-Petersen *et al.*, 2009).   Despite their importance, little information is available for life cycle of copepods other than dominant species.   For dominant copepods, their species-specific lipid accumulation and gonad maturation have little evaluated in the western Arctic Ocean.

In the present study, we analyzed zooplankton swimmers collected by sediment trap sampling at 13−15 day intervals moored at 184 m in Northwind Abyssal Plain during October 2010 to September 2011.   Through this analysis, seasonal changes in swimmer community structure and population structure of the four dominant copepods (*Calanus hyperboreus*, *Metridia longa*, *Paraeuchaeta glacialis* and *Heterorhabdus norvegicus*) were evaluated.   Lipid accumulation and gonad maturation of adult females (C6F) from the dominant copepods were analyzed to evaluate their life cycle patterns.   Seasonal occurrence of the Pacific copepods (*Neocalanus cristatus*) was also noted and the possible cause was discussed.

METHOD

Field sampling

Samples were collected by sediment trap (SMD26 S-6000, open mouth area 0.5 m^2, Nichiyu Giken Kogyo, Co. Ltd.) rotated at 13−15 day intervals moored at 184 m and 1,300 m at St. NAPt (Northwind Abyssal Plain trap, 75°00´N, 162°00´W, bottom depth 1975 m) during 4 October 2010 to 28 September 2011 (Fig. 1). This station is seasonally affected by inflow of Bering Shelf Water (BSW) from Bering Strait (Weingartner *et al.*, 2005; Woodgate *et al.*, 2005). The end of the trap rope was fixed to the sea bottom. Sea water for filling sample cups was taken from 1,000 m water depth in the southern Canada Basin (salinity 34.89), and was filtered with membrane filter (0.45 μm pore size) to make 5% buffered formalin seawater. The sample cups were filled with the 5% buffered formalin seawater before the sediment trap was deployed.

After the trap was retrieved, the 26 samples each were gently filtered with 1 mm mesh, and the remaining fraction (>1 mm size) on the mesh was treated as zooplankton swimmers. Since the number of zooplankton swimmer was low for deeper trap (1,300 m), we treated only shallower trap (184 m) in this study. The fine size fraction (<1 mm) for each sample was evenly divided to 10 aliquots using the Wet Sample Divider (McLane^{TM} WSD-10). The one of divided aliquots for each sample was filtered on weighed polycarbonate membrane filter, and was desalted with Milli-Q waters. The sample filters were dried with diphosphorus pentaoxide in desiccator for three days. The dried sample filters were weighed with analytical balance to calculate total mass flux (mg dry mass [DM] m^{-2} day^{-1}) of < 1 mm size fraction for each sample period.

As the supplemental environmental data, the moored trap depth and the water temperature (accuracy of ± 0.2°C) were monitored every hour (sensor type: ST-26S-T). We estimated the current speed at St. NAPt in 2010 by a physical ocean general circulation model: Center for Climate System Research Ocean Component Model (COCO) version 4.9. The model performance in the western Arctic Ocean has been verified in previous decadal and seasonal experiments (Watanabe *et al.*, 2012; Watanabe and Ogi, 2013). Time-series data on weekly averaged percentage ice coverage around St. NAPt (74.5−75.5°N, 161.5−162.5°W) during the mooring period were calculated from the sea ice concentration data set (http://iridl.ldeo.columbia.edu/SOURCES/.IGOS-

94   S/.nmc/.Reyn_SmithOIv2/, cf. Reynolds *et al.*, 2002).   For sea ice coverage data of whole Arctic

95   Ocean, the data were downloaded from the AMSER-E data set (http://www.ijis.iarc.uaf.edu/seaice/-

96   extent/plot.csv).   The MODIS/Aqua Level 3 binned chlorophyll-*a* data (reprocessing version

97   2012.0) were downloaded from the Distributed Active Archive Center (DAAC) of Goddard Space

98   Flight Center (GSFC), NASA.   We used daily data at 9-km resolution, and composited to 9 days

99   running mean.

100 **Analysis of zooplankton swimmer**

101 For zooplankton swimmer samples (>1 mm), identification and enumeration of zooplankton were

102 made under a dissecting microscope.   In this study, swimmer defined that zooplankton in >1 mm

103 samples swam actively into the trap (cf. Knauer *et al.*, 1979).   Specimens damaged before

104 collection were distinguished based on the description of Sampei *et al.* (2009), while their

105 contribution was small (<0.65% in total count) and excluded from following analysis.   Species

106 identification of copepods followed mainly Brodsky (1967) and Frost (1989) for *Pseudocalanus* spp.

107 (*P. minutus* and *P. newmani*), Frost (1974) for *Calanus* spp. (*C. glacialis* and *Calanus marshallae*),

108 and Miller (1988) for *Neocalanus* spp.   Identification of the four dominant calanoid copepods

109 (*Calanus hyperboreus*, *Metridia longa*, *Paraeuchaeta glacialis* and *Heterorhabdus norvegicus*) was

110 made to the copepodid stage level.

111   For *C. hyperboreus*, *M. longa* and *P. glacialis*, the copepodid stage 6 females (C6Fs)

112 contain a large oil sac in the prosome.   To analyze the amount of oil, oil length relative to prosome

113 length (PL) was scored into three groups: I (the lipid length is 0−4% of PL), II (4−40% of PL) and

114 III (>40% of PL).   For the same three species, gonad maturation of the C6F was also scored into

115 three groups: I (immature), II (small oocytes in ovary or oviduct) and III (large eggs or distended

116 opaque in oviduct).   For this gonad maturation index, we referred to those used previously for *C.*

117 *hyperboreus* (Hirche and Niehoff, 1996) and *M. longa* (Tande and Grønvik, 1983).   Of the four

118 dominant copepods, only *H. norvegicus* was not analyzed for lipid accumulation and gonad

119 maturation, because of the difficulty in observation.   *Heterorhabdus norvegicus* accumulate lipids

5

120 in many small oil droplets, and the low transparency of the prosome prevents observation of their

121 gonad.

122 The flux (F, ind. m^{-2} day^{-1}) of zooplankton swimmers was calculated from the following

123 equation:

124 $$F = N \times \frac{1}{0.5} \times \frac{1}{d}$$

125 where N is the number of individuals (ind.), 0.5 is the mouth area (m^2) of the sediment trap, and d is

126 the sampling interval (days). We counted total zooplankton swimmers 37−288 individuals per

127 sample. Since the sampling interval is similar (13−15 days) throughout the sampling period,

128 conversion factor between count and flux was similar (one individual sample^{-1} corresponded to

129 0.133−0.154 ind. m^{-2} day^{-1} [=1/0.5/13−15]).

130 **Data analysis**

131 Zooplankton swimmer flux data (F: ind. m^{-2} day^{-1}) for each species was log transformed

132 ($\log_{10}[X+1]$) prior to analysis to reduce the bias of flux. Similarities between samples were

133 examined using the Bray-Curtis index (Bray and Curtis, 1957). To group samples, the similarity

134 indices were coupled with hierarchical agglomerative clustering using a complete linkage method

135 (Unweighted Pair Group Method using Arithmetic mean: UPGMA) (Field *et al.*, 1982). All of

136 these analyses were carried out using PRIMER v6 software (PRIMER-E Ltd.). Inter-group

137 differences in flux of all zooplankton swimmers were tested by one-way ANOVA and an ex post

138 facto test by Fisher's Protected Least Significant Difference test (PLSD). These statistical

139 analyses were carried out using StatView v5 software (SAS Institute Inc.).

140 **RESULTS**

141 **Hydrography**

142 The trap depth varied between 181 and 218 m (Fig. 2a), and was stable around 184 m most of the

143 date then temporally deepened (220 m) within short period (6−7 days) in October, December 2010

144 and September 2011.　Temperature at sediment trap ranged from −1.6 to −0.6°C (Fig. 2b).　Rapid

145 decreases in temperature were paralleled with the deepening changes in the moored trap depth (Fig

146 2a, b).　The five days mean of current velocity simulated by ocean circulation model showed slow

147 subsurface current (<11.3 cm s^{-1} at 45 m and <2.7 cm s^{-1} at 188 m water depths) at St. NAPt (Fig.

148 2c).　From two times CTD casts at the station, four water masses were identified at 0−500 m water

149 column: i.e. SML: Surface Mixed Layer (0−25 m), PSW: Pacific Summer Water (25−100 m),

150 PWW: Pacific Winter Water (100−250 m), AW: Atlantic Water (>250 m) (Fig. 2d, e) (McLaughlin

151 *et al.*, 2011).

152 　　　Sea ice around the sediment-trap site showed clear seasonal changes, with a decrease from

153 early July, complete melting (sea ice concentration: 0%) in September, a rapid increase during

154 October, and 100% coverage during November to June (Fig. 3a).　The total mass flux (<1 mm size

155 range) ranged 19.3−215.9 mg DM m^{-2} day^{-1} and peaked during November−December (Fig. 3a).

156 High chl. *a* was observed during August−September (Fig. 3a).　At St. NAPt, the midnight sun

157 occurred during early May to early August, and polar night was from early November to early

158 February (Fig. 3b).

Swimmer community

160 Based on the zooplankton swimmer flux, cluster analysis classified the zooplankton swimmer

161 communities largely (A and B) at 55% dissimilarity level, then group B subdivided (B-1 and B-2) at

162 47% dissimilarity level (Fig. 4a).　Occurrence of each group showed distinct seasonality.　Group

163 A (*n* = 8) was observed from July to October, group B-1 (*n* = 6) from November to January, and

164 group B-2 (*n* = 9) from March to June (Fig. 4b).　Zooplankton swimmer flux ranged from 5 to 44

165 ind. m^{-2} day^{-1}.　While except extremely high peak of amphipods (*Themisto libellula*) in April,

166 zooplankton swimmer flux was highest during July to October (Fig. 4b).　The averaged

167 zooplankton swimmer flux was highest in A (20.0±4.9 ind. m^{-2} day^{-1}), lower in B-2 (16.1±3.9), and

168 lowest in B-1 (11.9±2.4).　Copepods comprised 18 to 94% of the zooplankton swimmer flux and

169 were the dominant taxon; amphipods the second most dominant group (0−74%) (Fig. 4b).　The

7

characterized species of each group (significantly abundant than the other groups analyzed by one-way ANOVA and Fisher's PLSD, $p<0.05$) were as follows: A, the mesopelagic copepods *Paraeuchaeta glacialis*; and B-2, the inter-zonal copepod *Calanus hyperboreus*. While group B-1 dominated by *Metridia longa* and *Heterorhabdus norvegicus*, their flux showed no significant seasonal changes.

Copepod population structure

The population structures of the four dominant copepods (*C. hyperboreus*, *M. longa*, *P. glacialis* and *H. norvegicus*) varied with species. Throughout the year, *C. hyperboreus* was predominated by C6F (Fig. 5a). The population structure of *M. longa* and *P. glacialis* showed seasonal change; both were dominated by C6F from January to May, and early copepodid stages (C1−C4) occurred during June−October (Fig. 5b, c). *Heterorhabdus norvegicus* showed a different seasonal pattern; it was dominated by C5 during November−February, the contribution of C6F/M increased during March−October, and C1 and C2 stages occurred in June−July (Fig. 5d).

Lipid accumulation in C6Fs of the dominant copepods (excluding *H. norvegicus*) also showed species-specific seasonal patterns. Most *C. hyperboreus* contained more lipids (stage III) during December−January (83%) than during February−October (56%) (Fig. 6a). For *M. longa,* stage III individuals dominated during October−December, their composition gradually decreased during March to June, and all specimens had no oil sacs in July (Fig. 6b). The lipid accumulation of *P. glacialis* showed fluctuated seasonal change (Fig. 6c).

Gonad maturation of C6Fs of the dominant copepods (excluding *H. norvegicus*) showed more distinct seasonality. For *C. hyperboreus*, mature individuals were observed only during February−April (Fig. 6d). Mature *M. longa* were seen during March−July, note that in September was based on only one specimen (Fig. 6e), with the lipid accumulation decreased (Fig. 6b). Most *P. glacialis* (47%) matured during August−January (Fig. 6f), when egg carrying *P. glacialis* C6Fs were also seen.

8

Pacific copepods

The Pacific copepod *Neocalanus cristatus* occurred ($0-0.92$ ind. m^{-2} day^{-1}) throughout the year, and was higher during August−September when the sea ice was reduced (Fig. 7).   All *N. cristatus* were stage C5, and lipid accumulation varied.

DISCUSSION

Trap collection efficiency

In general, underestimate bias in sinking particle flux is concerned due to low trap collection efficiency under flowing water condition especially shallower than 1,000 m (Buesseler *et al.*, 2007). The time-series monitoring data for physical oceanography around St. NAPt are limited.   However, the directly measured water current around St. NAPt in winter was slower than 10 cm s^{-1} at 58 and 250 m water depths (Sumata and Shimada, 2007).   The current speed estimated by ocean circulation model also confirmed that the speed of the subsurface current around trap was slow (<2.7 cm s^{-1}) at St. NAPt throughout the year (Fig. 2c).   These slow current speeds were not expected to have a significant effect on sediment trap collection efficiency.   The sediment trap temporarily deepened to 220 m with short period (6−7 days) in October, December 2010 and September 2011 (Fig. 2a).   Temporal changes in temperature also confirmed these changes (Fig. 2b).   The tilt of sediment trap was estimated within 15° in the deepening events.   Except for these periods, mooring depth of sediment trap was kept 180−190 m.   Since the PWW were occurred between 100−250 m (Fig. 2d, e), there expected little changes in water masses at the trap depth. Although the deployment depth of sediment trap was not completely constant throughout the studied period, the seasonality of total mass fluxes at 184 m trap and at 1,300 m trap (Onodera *et al.*, pers. comm.) was well paralleled ($r^2 = 0.621$, $p<0.0001$).   These results suggest that the influence of the trapping efficiency bias is usually insignificant for the studied sediment trap samples.

Seasonal changes in swimmer community

Previously reported zooplankton swimmer communities collected by sediment trap in the Arctic

Ocean are summarized in Table 1. Throughout the studies, copepods are the most dominant taxa, followed by amphipods or pteropods similar with this study. Within the copepods, *C. finmarchicus* is reported to be dominated for the shallower trap (ca. 100 m) in the Norwegian fjord faced to the North Atlantic Ocean (Willis *et al.*, 2006, 2008). While in the deep-layer (500 m) of the eastern Greenland Sea, *C. finmarchicus* was lesser and dominated by *M. longa* (Seiler and Brandt, 1997). For the western Arctic Ocean (Amundsen Gulf and Beaufort Sea), not faced to the Atlantic Ocean, *C. finmarchicus* did not occur and *M. longa* was dominated (Forbes *et al.*, 1992; Sampei *et al.*, 2012). For the northernmost station (81°N), diapausing *C. hyperboreus* was predominated (Hargrave *et al.*, 1989). Thus, the dominant copepod species collected by sediment trap may vary with region and trap depths. The trap depth of this study (184 m) was relatively shallow, but because the NAPt is not faced to the Atlantic Ocean, *C. finmarchicus* did not occur. Dominant copepods of this study, *H. norvegicus* followed with *M. longa*, were a unique, because of the dominance of the mesopelagic copepods (Yamaguchi and Ikeda, 2000). *Heterorhabdus norvegicus* is reported to be the second dominant copepods in the zooplankton swimmer fauna of the eastern Greenland Sea (Seiler and Brandt, 1997), thus this species may be dominant copepods throughout the mesopelagic layer of the Arctic Ocean. Copepod fauna evaluated by stratified net samplings also noted the occurrence of *H. norvegicus* throughout the Arctic Ocean (Kosobokova and Hirche, 2000; Auel and Hagen, 2002; Kosobokova and Hopcroft, 2010; Dvoretsky and Dvoretsky 2011). Add to these copepods, occurrence of small number of the Pacific copepods is a special feature of this study. Since the zooplankton swimmer community of this study showed clear seasonal changes (groups A, B-1 and B-2), following, we discuss the characteristics of each swimmer group.

The group A, corresponded with open water period (July−October), dominated by the carnivorous *P. glacialis* (3.7−9.4 times greater flux than the other groups, one-way ANOVA, $p < 0.001$). For the numerical dominance of *P. glacialis* during July−October, two factors are considered: i) correspondence of growth to large copepodid stages (>1 mm in size), ii) correspondence of presence of massive diel vertical migration (DVM) at that period. For the

former, dominance of C5 stage during the period (Fig. 5c) suggests that the major population grew up this season.   For the latter, *P. norvegica*, which is an Atlantic congener species for *P. glacialis*, is known to perform DVM during autumn (Kaartvedt *et al.*, 2002), but cease DVM during midnight sun and polar night (Fleddum *et al.*, 2001).   At St. NAPt, the midnight sun occurred during early May to early August, and polar night was from early November to early February (Fig. 3c).   Thus, if *P. glacialis* had similar DVM of *P. norvegica*, the dominance of *P. glacialis* in group A (July−October) was caused by the presence of DVM for *P. glacialis* during that period.

Changes in zooplankton swimmer community from group A to B-1 was corresponded with the timing of ice coverage and entered polar night (Fig. 3c).   The group B-1 was characterized with the dominance of mesopelagic *M. longa* and *H. norvegicus*.   While their flux showed little seasonal changes (Fig. 5b, d), the other two species showed clear seasonality: peaked in May−June for *C. hyperboreus* (Fig. 5a) and July−October for *P. glacialis* (Fig. 5c).   Thus, group B-1 was composed mainly by mesopelagic copepods (*M. longa* and *H. norvegicus*) stable occurred in the mesopelagic layer.   For the other two species (*C. hyperboreus* and *P. glacialis*), seasonal vertical migration (SVM) and presence/absence of DVM is considered to be a key mechanism to govern the seasonal changes in swimmer community.

During the ice coverage period (November−June), the swimmer community changed from group B-1 to B-2 in February due to the drastic increase (ca. 10 times) of *C. hyperboreus* (one-way ANOVA, $p<0.01$).   *Calanus hyperboreus* is known to perform SVM (Hirche, 1997; Vinogradov, 1997), diapause at depth (500−1,500 m) in winter, and make upward SVM to the surface layer in April (Hirche and Niehoff, 1996).   In the present study, it was shown that *C. hyperboreus* included only C6Fs and their flux increased from February and peaked in May (Fig. 5a).   This increase in flux during February to May was presumably due to their upward SVM from deep layer. Therefore, the change in swimmer community (from group B-1 to B-2) during January−March might have been caused by the upward SVM of *C. hyperboreus*.   For arousal mechanism of resting copepods, presence of an internal body timer is discussed (Miller and Grigg, 1991; Miller *et al.*, 1991).   Since daylight hours changed greatly from zero (polar night) to 24h (midnight sun) during

11

274   February to April (Fig. 3c), this change in day-night cycle may affect the arousal of diapause for *C.*

275   *hyperboreus*.

276   As specialized seasonal event of this study, the occurrence of Pacific copepods was

277   observed.   The Pacific copepod *N. cristatus* C5 was abundant during August−September when sea

278   ice coverage decreased (Fig. 8).   This seasonal pattern suggests that the amount of the inflow

279   Pacific Water may increase when the sea ice coverage decreases.   While *N. cristatus* C5 is known

280   to perform SVM to deep layer to diapause during late summer (Miller *et al.*, 1984), the greater flux

281   of *N. cristatus* C5 in August−September may also be caused by their SVM.   Since their

282   reproduction occurs >1,000 m depth (Miller *et al.*, 1984), the possibility of their reproduction in the

283   Arctic Ocean could not be evaluated from this study.

284   **Population structure of dominant copepods**

285   *Calanus hyperboreus* populations were composed much of C6F throughout the year (Fig. 5a).

286   *Calanus hyperboreus* reproduces during November−April in Amundsen Gulf (Ota *et al.*, 2008),

287   November−March in the Greenland Sea (Hirche and Niehoff, 1996), and February−March in the

288   Norwegian Sea (Østvedt, 1955).   In the present study, mature C6F were seen only from February

289   to April, which suggests this is the reproduction period (Fig. 8).   This reproduction season

290   (February−April) generally corresponds to the previous studies with slight seasonal variances.   For

291   the regional variability in reproduction timing of *C. hyperboreus*, timing of the phytoplankton

292   bloom is reported to be a most important factor (Conover and Siferd, 1993; Hirche and Niehoff,

293   1996).   Full-lipid individuals in stage C6F dominated in December−January, and the lipid

294   accumulation decreased from February when the reproduction started (Fig. 6a).   This seasonal

295   correspondence between reproduction period and decrease of lipid accumulation would be caused

296   by the utilization of the stored lipid to reproduction (Hirche and Niehoff, 1996; Vinogradov, 1997).

297   The *M. longa* population was dominated by C6F during January−May, and early copepodid

298   stages (C1−C4) during June−October (Fig. 5b).   *Metridia longa* is omnivore and performs diel

299   vertical migration (Conover and Huntley, 1991; Ashjian *et al.*, 1995), and has no diapause phase

(Båmstedt and Ervik, 1984; Grønvik and Hopkins, 1984). The main reproduction season shows regional variability: during April−May in the Balsfjorden (Tande and Grønvik, 1983), in winter under the sea ice in the Barents Sea (Hirche and Kosobokova, 2011), and in autumn in a polynya in the Beaufort Sea (Makabe *et al.*, 2010). In this study, mature C6F occurred only during March−July (Fig. 6e), and early copepodid stages (C1−C4) dominated the population during June−October (Fig. 5b). These facts suggest that *M. longa* reproduces during March−July and the new population appear during June−October. This reproduction season (March−July) in the western Arctic Ocean is slightly longer than that in the Balsfjorden (April−May) (Tande and Grønvik, 1983). Lipid accumulated (stage III) individuals dominated during October−December, decreased gradually over winter and no specimens had oil sacs in July (Fig. 6b). This season of decreasing lipids (March−June) parallels the gonad maturation season (March−July). These facts suggest that the stored lipids are used for gonad maturation of *M. longa* as was seen in *C. hyperboreus*.

The *P. glacialis* population was dominated by C6F during January−May, and contained early copepodid stages (C2−C4) during June−October (Fig. 5c). Carnivorous *Paraeuchaeta* spp. performs raptorial feeding throughout the year, accumulate much lipids, and have no diapause phase (Båmstedt, 1979; Øresland, 1991). Since mature C6F *P. glacialis* dominated during August−January and egg carrying C6F also occurred during the same period (Fig. 6f), this species is assumed to reproduce in this period. This may be related to the ice-edge bloom at the surface. Ice-edge bloom is known to be occurred after ice melting (Springer and McRoy, 1993) (Fig. 3b). Ice-edge bloom induces the upward migration of Arctic copepods (e.g., *C. glacialis*) and reproduction of small copepods (e.g., *Pseudocalanus* spp.) (Conover and Huntley, 1991), which would provide sufficient food condition for carnivorous *P. glacialis*. Since sufficient food condition (abundant small metazoan zooplankton) is a key to make growth and reproduction of *Paraeuchaeta* spp. (Yamaguchi and Ikeda, 2001; Abe *et al.*, 2012), *P. glacialis* may have performed reproduction in this season. This reproduction season of *P. glacialis* (August−January) differs with those of *C. hyperboreus* (February−April) and *M. longa* (March−July). These differences

327 may be related to differences in feeding modes, i.e., carnivory in *P. glacialis* and suspension feeding

328 in *C. hyperboreus* and *M. longa*.

329   The *H. norvegicus* population was dominated by C5 during November−February and

330 C6F/M during March−October, and C1 and C2 were collected in June and July (Fig. 5d).   Since

331 lipid accumulation and gonad maturation could not be analyzed for *H. norvegicus*, the reproduction

332 season was estimated from the population structure data.   Combining dominance of early

333 copepodid stage (June and July) and assuming development time of *Heterorhabdus* spp. nauplii

334 (1−2 months) (Yamaguchi and Ikeda, 2000), the reproduction season is thought to be during April

335 and May.   Little comparable information is available for the life cycle of *H. norvegicus*.   Thus,

336 the reproduction seasons of the dominant four copepods differed (Fig. 8), and possible causes of

337 these differences include species-specific feeding modes, seasonal changes in food availability, and

338 the presence/absence of ontogenetic vertical migration.

339   In summary, while the limitation of sampling design (data based on single sediment trap at

340 a single station and depth), through the analyses on zooplankton swimmers collected by a sediment

341 trap, zooplankton communities were clearly separated into three seasons (Fig. 8).   The season

342 when each copepod dominated corresponded with the reproduction timing of each species.   For the

343 four dominant copepods, their reproduction timings varied with species, which may be related to the

344 feeding modes.   In addition, the occurrence of the Pacific copepods was observed.   Since their

345 peak period (August−September) corresponded with timing of their SVM, they may enter sediment

346 trap to perform descent SVM.

353 manuscript.

362 **REFERENCES**

363 Abe, Y., Ishii, K., Yamaguchi, A. *et al.* (2012) Short-term changes in population structure and

364   vertical distribution of mesopelagic copepods during the spring phytoplankton bloom in

365   the Oyashio region. *Deep-Sea Res. I*, **65**, 100−112.

366 Ashjian, C.J., Smith, S.L. and Lane, P.V.Z. (1995) The Northeast Water Polynya during summer

367   1992: distribution and aspects of secondary production of copepods. *J. Geophys. Res.*, **100**,

368   4371−4388.

369 Auel, H. and Hagen, W. (2002) Mesozooplankton community structure, abundance and biomass in

370   the central Arctic Ocean. *Mar. Biol.*, **140**, 1013−1021.

371 Båmstedt, U. (1979) Reproduction bioenergetics within the summer and winter generations of

372   *Euchaeta norvegica* (Copepoda). *Mar. Biol.*, **54**, 135−142.

373 Båmstedt, U. and Ervik, A. (1984) Local variations in size and activity among *Calanus*

374   *finmarchicus* and *Metridia longa* (Copepoda, Calanoida) overwintering on the west coast

375   of Norway. *J. Plankton Res.*, **6**, 843−857.

376 Bray, J.B. and Curtis, J.T. (1957) An ordination of the upland forest communities of southern

377   Wisconsin. *Ecol. Monogr.*, **27**, 325−349.

378 Brodsky, K.A. (1967) *Calanoida of the Far-eastern Seas and Polar Basin of the USSR*. Israel

379   Program Scientific Translation, Jerusalem.

380 Buesseler, K.O., Antia, A.N., Chen, M. *et al.* (2007) An assessment of the use of sediment traps for

381   estimating upper ocean particle fluxes. *J. Mar. Res.*, **65**, 345−416.

382 Comiso, J.C., Parkinson, C.L., Gersten, R. *et al.* (2008) Accelerated decline in the Arctic sea ice

383   cover. *Geophys. Res. Lett.*, **35**, L01703, doi: 10.1029/2007GL031972.

384 Conover, R.J. and Huntley, M. (1991) Copepods in ice-covered seas−Distribution, adaptations to

385   seasonally limited food, metabolism, growth patterns and life cycle strategies in polar seas.

386   *J. Mar. Syst.*, **2**, 1−41.

387 Conover, R.J. and Siferd, T.D. (1993) Dark-season survival strategies of coastal zone zooplankton

388   in the Canadian Arctic. *Arctic*, **46**, 303−311.

389 Darnis, G., Barber, D.G. and Fortier, L. (2008) Sea ice and the onshore−offshore gradient in

390   pre-winter zooplankton assemblages in southeastern Beaufort Sea. *J. Mar. Syst.*, **74**,

391   994−1011.

392 Dvoretsky, V.G. and Dvoretsky, A.G. (2011) Copepod communities off Franz Josef Land (northern

393   Barents Sea) in late summer of 2006 and 2007. *Polar Biol.*, **34**, 1231−1238.

394 Falk-Petersen, S., Mayzaud, P. and Kattner, G. (2009) Lipids and life strategy of Arctic *Calanus*.

395   *Mar. Biol. Res.*, **5**, 18−39.

396 Field, J.G., Clarke, K.R. and Warwick, R.M. (1982) A practical strategy for analyzing multispecies

397   distribution patterns. *Mar. Ecol. Prog. Ser.*, **8**, 37−52.

398 Fleddum, A., Kaartvedt, S. and Ellertsen, B. (2001) Distribution and feeding of the carnivorous

399   copepod *Paraeuchaeta norvegica* in habitats of shallow prey assemblages and midnight

400   sun. *Mar. Biol.*, **139**, 719−726.

401 Forbes, J.R., Macdonald, R.W., Carmack, E.C. *et al.* (1992) Zooplankton retained in sequential

402   sediment traps along the Beaufort Sea shelf break during winter. *Can. J. Fish. Aquat. Sci.*,

403   **49**, 663−670.

404 Frost, B.W. (1974) *Calanus marshallae*, a new species of calanoid copepod closely allied to the

405   sibling species *C. finmarchicus* and *C. glacialis*. *Mar. Biol.*, **26**, 77−99.

406 Frost, B.W. (1989) A taxonomy of the marine calanoid copepod genus *Pseudocalanus*. *Can. J. Zool.*,

407   **67**, 525−551.

408 Grebmeier, J.M. (2012) Shifting patterns of life in the Pacific Arctic and sub-Arctic Seas. *Annu. Rev.*

409   *Mar. Sci.*, **4**, 63−78.

410 Grebmeier, J.M., Cooper, L.W., Feder, H.M. *et al.* (2006) Ecosystem dynamics of the

411   Pacific-influenced northern Bering and Chukchi Seas in the Amerasian Arctic. *Prog.*

412   *Oceanogr.*, **71**, 331–361.

413 Grønvik, S. and Hopkins, C.C.E. (1984) Ecological investigations of the zooplankton community of

414   Balsfjorden, northern Norway: generation cycle, seasonal vertical distribution, and

415   seasonal variations in body weight and carbon and nitrogen content of the copepod

416   *Metridia longa* (Lubbock). *J. Exp. Mar. Biol. Ecol.*, **80**, 93−107.

417   Hargrave, B.T., Bodungen B., Conover, R.J. *et al.* (1989) Seasonal changes in sedimentation of

418   particulate matter and lipid content of zooplankton collected by sediment trap in the Arctic

419   Ocean off Axel Heiberg Island. *Polar Biol.*, **9**, 467−475.

420   Hirche, H.-J. (1997) Life cycle of the copepod *Calanus hyperboreus* in the Greenland Sea. *Mar.*

421   *Biol.*, **128**, 607−618.

422   Hirche, H.-J. and Kosobokova, K.N. (2011) Winter studies on zooplankton in Arctic seas: the

423   Storfjord (Svalbard) and adjacent ice-covered Barents Sea. *Mar. Biol.*, **158**, 2359−2376.

424   Hirche, H.-J. and Niehoff, B. (1996) Reproduction of the Arctic copepods *Calanus hyperboreus* in

425   the Greenland sea-field and laboratory observations. *Polar Biol.*, **16**, 209−219.

426   Hopcroft, R.R., Kosobokova, K.N. and Pinchuk, A.I. (2010) Zooplankton community patterns in

427   the Chukchi Sea during summer 2004. *Deep-Sea Res. II*, **57**, 27−39.

428   Hunt, Jr.G.L. and Drinkwater, K. (2007) Introduction to the proceedings of the GLOBEC

429   symposium on effects of climate variability on sub-Arctic marine ecosystems. *Deep-Sea*

430   *Res. II*, **54**, 2453−2455.

431   Kaartvedt, S., Dale, T., Bagøien, E. *et al.* (2002) Bi-modal vertical distribution of the carnivorous

432   copepod *Paraeuchaeta norvegica*. *J. Plankton Res.*, **24**, 155−158.

433   Knauer, G.A., Martin, J.H. and Bruland, K.W. (1979) Fluxes of particulate carbon, nitrogen, and

434   phosphorus in the upper water column of the northeast Pacific. *Deep-Sea Res.*, **26A**,

435   97−108.

436   Kosobokova, K.N. and Hirche, H.-J. (2000) Zooplankton distribution across the Lomonosov Ridge,

437   Arctic Ocean: species inventory, biomass and vertical structure. *Deep-Sea Res. I*, **47**,

438   2029−2060.

439   Kosobokova, K.N. and Hopcroft, R.R. (2010) Diversity and vertical distribution of

440   mesozooplankton in the Arctic's Canada Basin. *Deep-Sea Res. II*, **57**, 96−110.

441   Makabe, R., Hattori, H., Sampei, M. *et al.* (2010) Regional and seasonal variability of zooplankton

442   collected using sediment trap in the southeastern Beaufort Sea, Canadian Arctic. *Polar*

443   *Biol.*, **33**, 257−270.

444   Markus, T., Stroeve, J.C. and Miller, J. (2009) Recent changes in Arctic sea ice melt onset, freezeup,

445   and melt season length. *J. Geophys. Res.*, **114**, C12024. doi: 10.1029/2009JC005436.

446   Matsuno, K., Yamaguchi, A., Hirawake, T. *et al.* (2011) Year-to-year changes of the

447   mesozooplankton community in the Chukchi Sea during summers of 1991, 1992 and 2007,

448   2008. *Polar Biol.*, **34**, 1349−1360.

449   Matsuno, K., Yamaguchi, A., Shimada, K. *et al.* (2012) Horizontal distribution of calanoid copepods

450   in the western Arctic Ocean during the summer of 2008. *Polar Sci.*, **6**, 105−119.

451   McLaughlin, F., Carmack, E., Proshutinsky, A. *et al.* (2011) The rapid response of the Canada Basin

452   to climate forcing: From bellwether to alarm bells. *Oceanography*, **24**, 146−159,

453   http://dx.doi.org/10.5670/oceanog.2011.66.

454   Miller, C.B. (1988) *Neocalanus flemingeri*, a new species of calanidae (copepoda: calanoida) from

455   the subarctic Pacific Ocean, with a comparative redescription of *Neocalanus plumchrus*

456   (Marukawa) 1921. *Prog. Oceanogr.*, **20**, 223−273.

457   Miller, C.B. and Grigg, H. (1991) An experimental study of the resting phase in *Calanus*

458   *finmarchicus* (Gunnerus). *Bull. Plankton Soc. Japan*, **special volume**, 479−493.

459   Miller, C.B., Cowles, T.J., Wiebe, P.H. *et al.* (1991) Phenology in *Calanus finmarchicus*;

460   hypotheses about control mechanisms. *Mar. Ecol. Prog. Ser.*, **72**, 79−91.

461   Miller, C.B., Frost, B.W., Batchelder, H.P. *et al.* (1984) Life histories of large, grazing copepods in

462   the subarctic ocean gyre: *Neocalanus plumchrus*, *Neocalanus cristatus* and *Eucalanus*

463   *bungii* in the Northeast Pacific. *Prog. Oceanogr.*, **13**, 201–243.

464   Øresland, V. (1991) Feeding of the carnivorous copepod *Euchaeta antarctica* in Antarctic waters.

465   *Mar. Ecol. Prog. Ser.*, **78**, 41–47.

466   Østvedt, O.J. (1955) Zooplankton investigations from weathership "M" in the Norwegian Sea,

467   1948−49. *Hvalrad. Skr.*, **40**, 1−93.

468   Ota, Y., Hattori, H., Makabe, R. *et al.* (2008) Seasonal changes in nauplii and adults of *Calanus*

469   *hyperboreus* (Copepoda) captured in sediment trap, Amundsen Gulf, Canadian Arctic.

470   *Polar Sci.*, **2**, 215−222.

471 Reynolds, R.W., Rayner, N.A., Smith, T.M. *et al.* (2002) An improved in situ and satellite SST

472   analysis for climate. *J. Clim.*, **15**, 1609−1625.

473 Sampei, M., Sasaki, H., Hattori, H. *et al.* (2009) Significant contribution of passively sinking

474   copepods to the downward export flux in Arctic waters. *Limnol. Oceanogr.*, **54**,

475   1894−1900.

476 Sampei, M., Sasaki, H., Forest, A. *et al.* (2012) A substantial export flux of particulate organic

477   carbon linked to sinking dead copepods during winter 2007−2008 in the Amundsen Gulf

478   (southeastern Beaufort Sea, Arctic Ocean). *Limnol. Oceanogr.*, **57**, 90−96.

479 Seiler, D. and Brandt, A. (1997) Seasonal occurrence of plankton Crustacea in sediment trap

480   samples at three depth horizons in the Greenland Sea. *Polar Biol.*, **17**, 337−349.

481 Shimada, K., Carmack, E.C., Hatakeyama, K. *et al.* (2001) Varieties of shallow temperature

482   maximum waters in the western Canadian Basin of the Arctic. *Geophys. Res. Lett.*, **28**,

483   3441−3444.

484 Shimada, K., Kamoshida, T., Itoh, M. *et al.* (2006) Pacific Ocean inflow: Influence on catastrophic

485   reduction of sea ice cover in the Arctic Ocean. *Geophys. Res. Lett.*, **33**, L08605, doi:

486   10.1029/2005GL0256254.

487 Springer, A.M. and McRoy, C.P. (1993) The paradox of pelagic food webs in the northern Bering

488   Sea-III. Patterns of primary production. *Cont. Shelf Res.*, **13**, 575−599.

489 Springer, A.M., McRoy, C.P. and Turco, K.R. (1989) The paradox of pelagic food web in the

490   northern Bering Sea-II. Zooplankton communities. *Cont. Shelf Res.*, **9**, 359−386.

491 Stroeve, J., Holland, M.M., Meier, W. *et al.* (2007) Arctic sea ice decline: Faster than forecast.

492   *Geophys. Res. Lett.*, **34**, L09501. doi: 10.1029/2007GL029703.

493 Sumata, H. and Shimada, K. (2007) Northward transport of Pacific summer water along the

494   Northwind Ridge in the western Arctic Ocean. *J. Oceanogr.*, **63**, 363−378.

495 Tande, K.S. and Grønvik, S. (1983) Ecological investigations on the zooplankton community of

496   Balsfjorden, northern Norway: sex ratio and gonad maturation cycle in the copepod

Metridia longa (Lubbock). *J. Exp. Mar. Biol. Ecol.*, **71**, 43−54.

Vinogradov, M.E. (1997) Some problems of vertical distribution of meso- macroplankton in the ocean. *Adv. Mar. Biol.*, **32**, 1−92.

Watanabe, E. and Ogi, M. (2013) How does Arctic summer wind modulate sea ice-ocean heat balance in the Canada Basin? *Geophys. Res. Lett.*, **40**, 1569−1574, doi:10.1002/grl.50363.

Watanabe, E., Kishi, M.J., Ishida, A. *et al.* (2012) Western Arctic primary productivity regulated by shelf-break warm eddies. *J. Oceanogr.*, **68,** 703−718, doi:10.1007/s10872-012-0128-6.

Weingartner, T., Aagaard, K., Woodgate, R. *et al.* (2005) Circulation on the north central Chukchi Sea shelf. *Deep-Sea Res. II*, **52**, 3150−3174.

Willis, K.J., Cottier, F.R., Kwaśniewski, S. *et al.* (2006) The influence of advection on zooplankton community composition in an Arctic fjord (Kongsfjorden, Svalbard). *J. Mar. Syst.*, **61**, 39−54.

Willis, K.J., Cottier, F.R., Kwaśniewski, S. (2008) Impact of warm advection on the winter zooplankton community in an Arctic fjord. *Polar Biol.*, **31**, 475−481.

Woodgate, R.A., Aagaard K., Swift, J.H. *et al.* (2005) Pacific ventilation of the Arctic Ocean's lower halocline by upwelling and diapycnal mixing over the continental margin. *Geophys. Res. Lett.*, **32**, L18609, doi: 10.1029/2005GL023999.

Woodgate, R.A., Weingartner, T. and Lindsay, R. (2010) The 2007 Bering Strait oceanic heat flux and anomalous Arctic sea-ice retreat. *Geophys. Res. Lett.*, **37**, L01602. doi: 10.1029/2009GL041621.

Yamaguchi, A. and Ikeda, T. (2000) Vertical distribution, life cycle, and body allometry of two oceanic calanoid copepods (*Pleuromamma scutullata* and *Heterorhabdus tanneri*) in the Oyashio region, western North Pacific Ocean.   *J. Plankton Res.*, **22**, 29−46.

Yamaguchi, A. and Ikeda, T. (2001) Abundance and population structure of three mesopelagic *Paraeuchaeta* species (Copepoda: Calanoida) in the Oyashio region, western subarctic Pacific Ocean with notes on their carcasses and epizonic ciliates. *Plankton Biol. Ecol.*, **48**, 104−113.

Figure legends

Fig. 1. Location of St. NAPt (Northwind Abyssal Plain trap) in the western Arctic Ocean where the sediment trap was moored at 184 m during October 2010 to September 2011. ACW: Alaskan Coastal Water, AW: Anadyr Water, BSW: Bering Shelf Water.

Fig. 2. Seasonal changes in depth (a) and temperature (b) monitored for shallower trap at St. NAPt during October 2010 to September 2011. Current velocity at 45 m and 188 m of St. NAPt (c) estimated by a physical ocean general circulation model: Center for Climate System Research Ocean Component Model (COCO) version 4.9. Temperature (d) and salinity (e) observed from CTD casts at St. NAPt in 30 October 2010 and 21 September 2012. Shades indicate the trap depths (180−190 m). SML: Surface Mixed Layer (0−25 m), PSW: Pacific Summer Water (25−100 m), PWW: Pacific Winter Water (100−250 m), AW: Atlantic Water (>250 m).

Fig. 3. Seasonal changes in sea ice concentration for the investigation area during the sampling period (http://iridl.ldeo.columbia.edu/SOURCES/.IGOSS/.nmc/.Reyn_SmithOIv2/, data from Reynolds *et al.*, 2002), total mass flux (<1 mm size fraction) collected by sediment trap, surface chl. *a* from satellite (a) and daylight hours (b) at St. NAPt during 4 October 2010 to 28 September 2011.

Fig. 4. Results of cluster analysis based on the flux of zooplankton swimmers. Twenty six samples were clustered into three groups from Bray-Curtis dissimilarity (a). Seasonal changes in zooplankton swimmer flux, species composition and clustered groups collected by sediment trap moored at 184 m of St. NAPt during 4 October 2010 to 28 September 2011 (b).

Fig. 5. Seasonal changes in flux and copepodid stage composition of the four dominant copepods: *Calanus hyperboreus* (a), *Metridia longa* (b), *Paraeuchaeta glacialis* (c), *Heterorhabdus norvegicus* (d), at 184 m of St. NAPt during 4 October 2010 to 28 September 2011.

Fig. 6. Seasonal changes in flux, lipid accumulation (upper panels) and gonad maturation (lower panels) compositions (stage I−III) of C6Fs of *Calanus hyperboreus* (whole $n = 232$) (a, d),

551   *Metridia longa* ($n = 234$) (b, e) and *Paraeuchaeta glacialis* ($n = 166$) (c, f) at 184 m of St.

552   NAPt during 4 October 2010 to 28 September 2011. *: Egg sac attached individual was

553   occurred.

554 **Fig. 7.** Seasonal changes in flux and lipid accumulation composition (I−III) of the Pacific

555   *Neocalanus cristatus* C5 collected by sediment trap moored at 184 m of St. NAPt during 4

556   October 2010 to 28 September 2011.

557 **Fig. 8.** Schematic diagram on seasonal changes in daylight hours, sea ice concentration, chl. *a*,

558   total mass flux (upper panel), swimmer community, population structure and reproduction

559   period of copepods (*C. hyperboreus*, *M. longa*, *P. glacialis* and *H. norvegicus*), and

560   occurrences of the Pacific *N. cristatus* collected by sediment trap at 184 m of St. NAPt

561   during 4 October 2010 to 28 September 2011 (lower panel). For *C. hyperboreus*, *M.*

562   *longa* and *P. glacialis*, reproduction period was evaluated by C6F gonad maturation (Fig.

563   6d−f). For *H. norvegicus*, their reproduction period was estimated by the occurrence of

564   early copepodid stages (Fig. 5d).

Table 1. Comparison of zooplankton swimmer community collected by sediment trap in the Arctic Ocean.

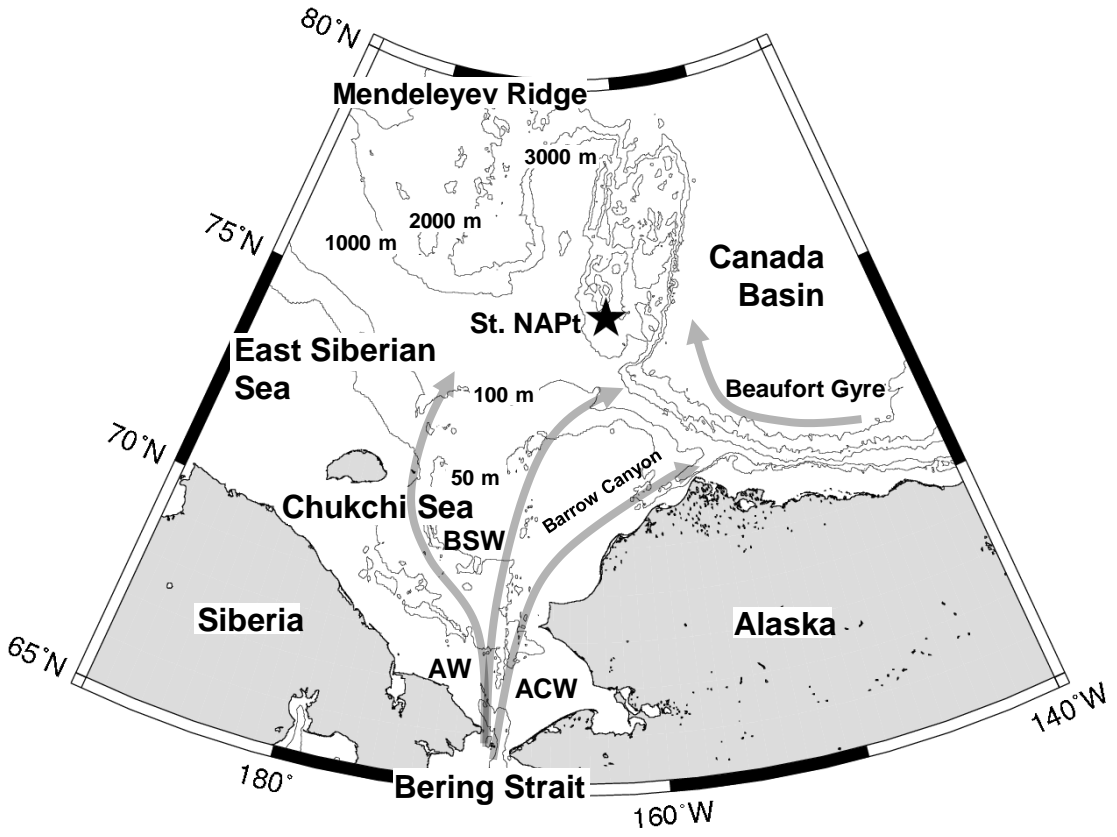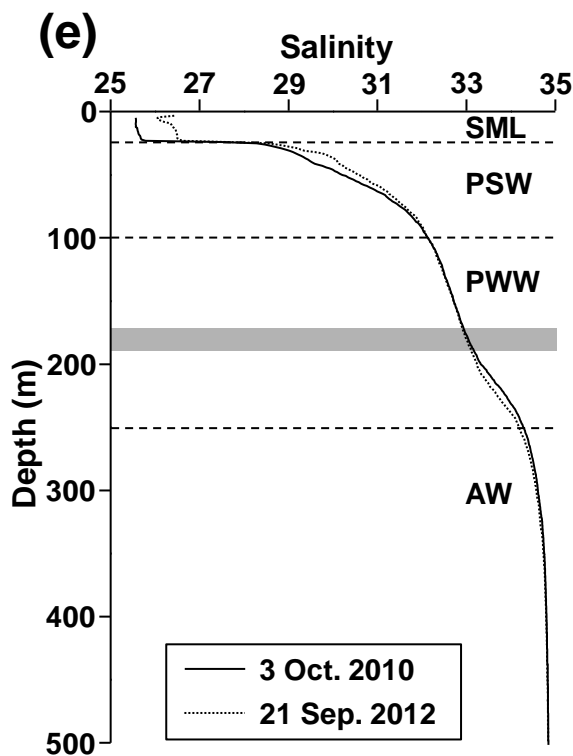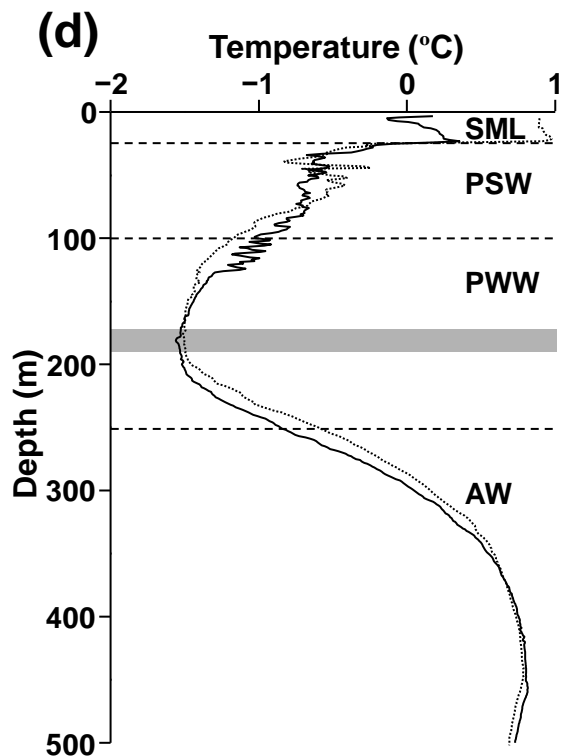| Region (position)	Period	Depth (m)	Dominant taxa/species (percentage to total zooplankton flux in number)	References
Amundsen Gulf (71°47′N, 126°30′W)	Oct. 2007–July 2008	112	*M. longa* (50), *P. glacialis* (6), *C. hyperboreus* (2), *C. glacialis* (2)	Sampei *et al.* (2012)
Amundsen Gulf (70–72°N, 123–135°W)	Oct. 2003–Aug. 2004	100, 200, 400	*Oncaea* spp. (34), *M. longa* (21), pteropods (11), *C. hyperboreus* (4)	Makabe *et al.* (2010)
Beaufort Sea Shelfbreak (69–72°N, 127–139°W)	Sep. 1987–Mar. 1988	115, 128, 145	*M. longa* (49), amphipods (27), *P. glacialis* (15), *C. hyperboreus* (8)	Forbes *et al.* (1992)
East Greenland Sea (72°0′–30 N, 7°2′–43 W)	July 1989–July 1992	500	*M. longa* (59), *H. norvegicus* (12), amphipods (9), ostracods (8)	Seiler and Brandt (1997)
Kongsfjorden (79°1.2′N, 11°46.41′E)	Sep. 2005–May 2006	115	*C. finmarchicus*, *C. glacialis*, *M. longa*, *P. norvegica*	Willis *et al.* (2008)
Kongsfjorden (79°3.2′N, 11°18.0′E)	Apr.–June, July–Sep. 2002	215	*C. finmarchicus*, *C. glacialis*, *C. hyperboreus*, *P. norvegica*	Willis *et al.* (2006)
Axel Heiberg Island (81°N, 96–98°W)	Sep. 1986–June 1987	100	*C. hyperboreus* (78), *M. longa* (9), *P. norvegica* (4), *C. glacialis* (2)	Hargrave *et al.* (1989)
Northwind Abyssal Plain (75°47′N, 126°30′W)	Oct. 2010–Sep. 2011	180	*H. norvegicus* (17), *M. longa* (16), *P. glacialis* (15), *C. hyperbpreus* (8)	This study

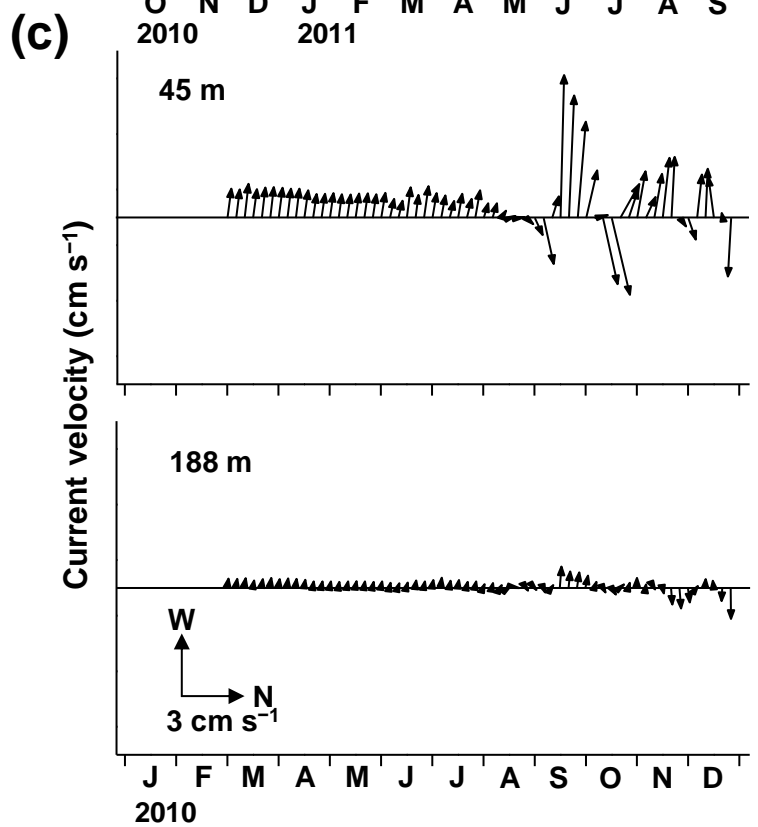Fig. 1 (Matsuno et al.)

(a)

(b)

(c)

(d) Temperature (°C)

(e) Salinity
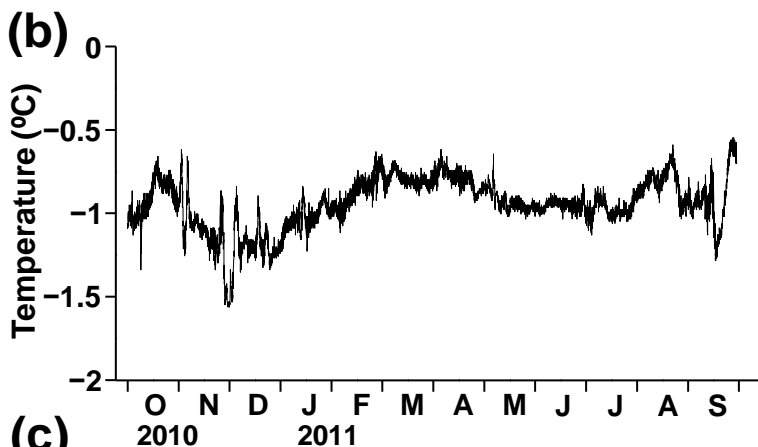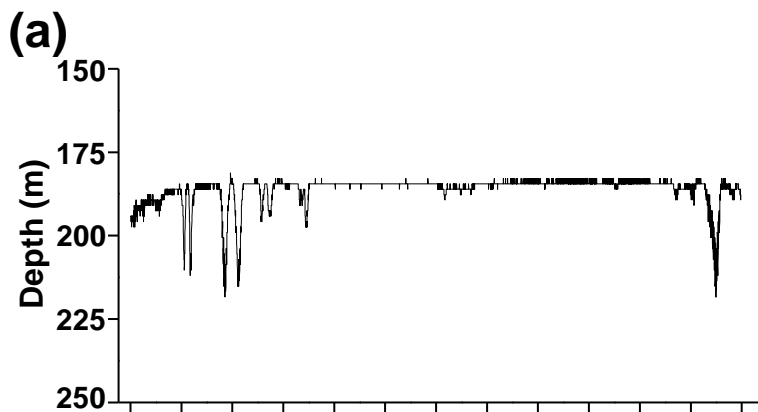
Fig. 2 (Matsuno et al.)

Fig. 3 (Matsuno et al.)

(a)

(b)

Fig. 4 (Matsuno et al.)

(a) *C. hyperboreus*

(b) *M. longa*

(c) *P. glacialis*

(d) *H. norvegicus*

Flux (ind. m⁻² day⁻¹)

Composition (%)

O N D J F M A M J J A S
2010   2011

O N D J F M A M J J A S
2010   2011

Flux   C1   C2   C3   C4   C5   C6F   C6M
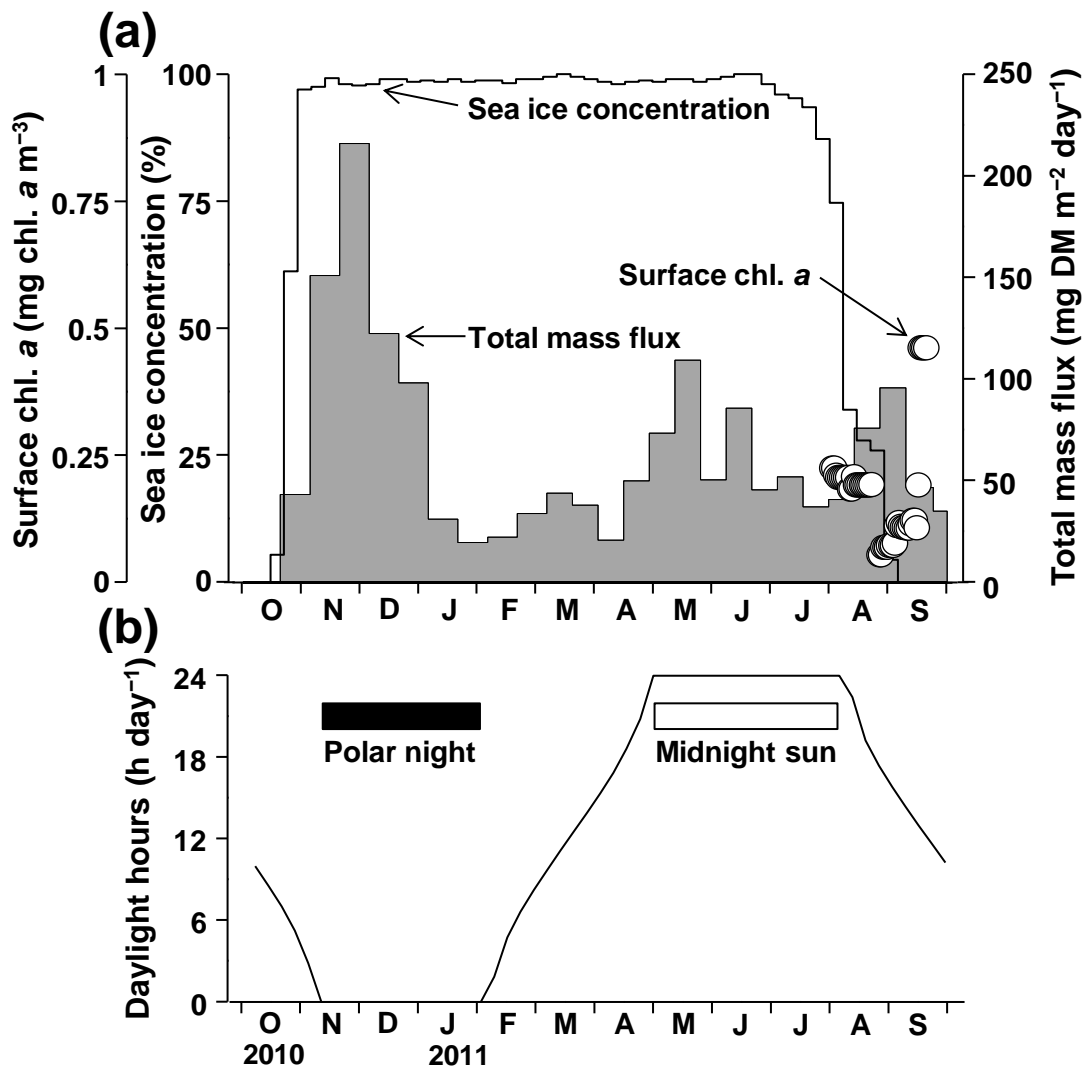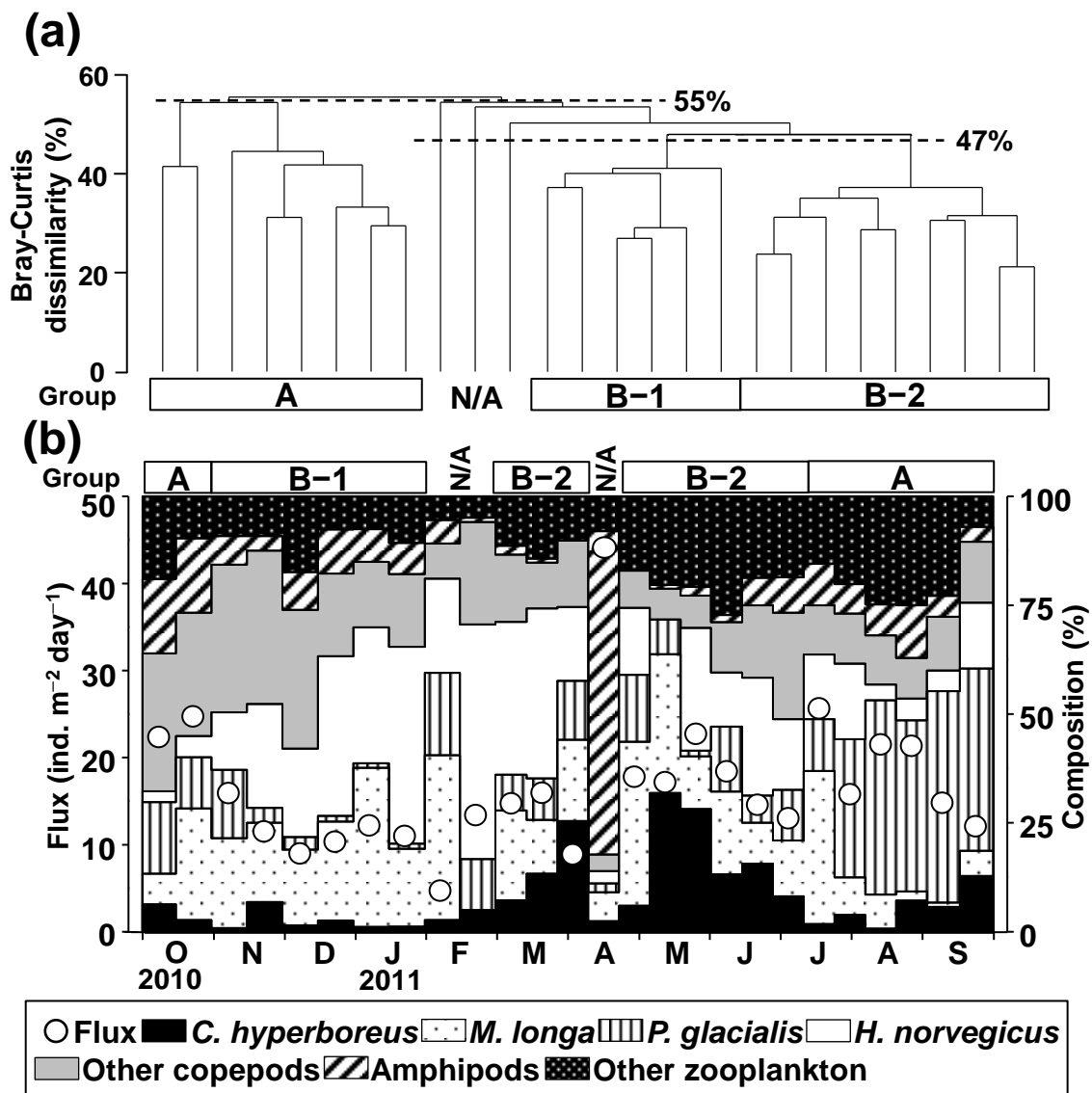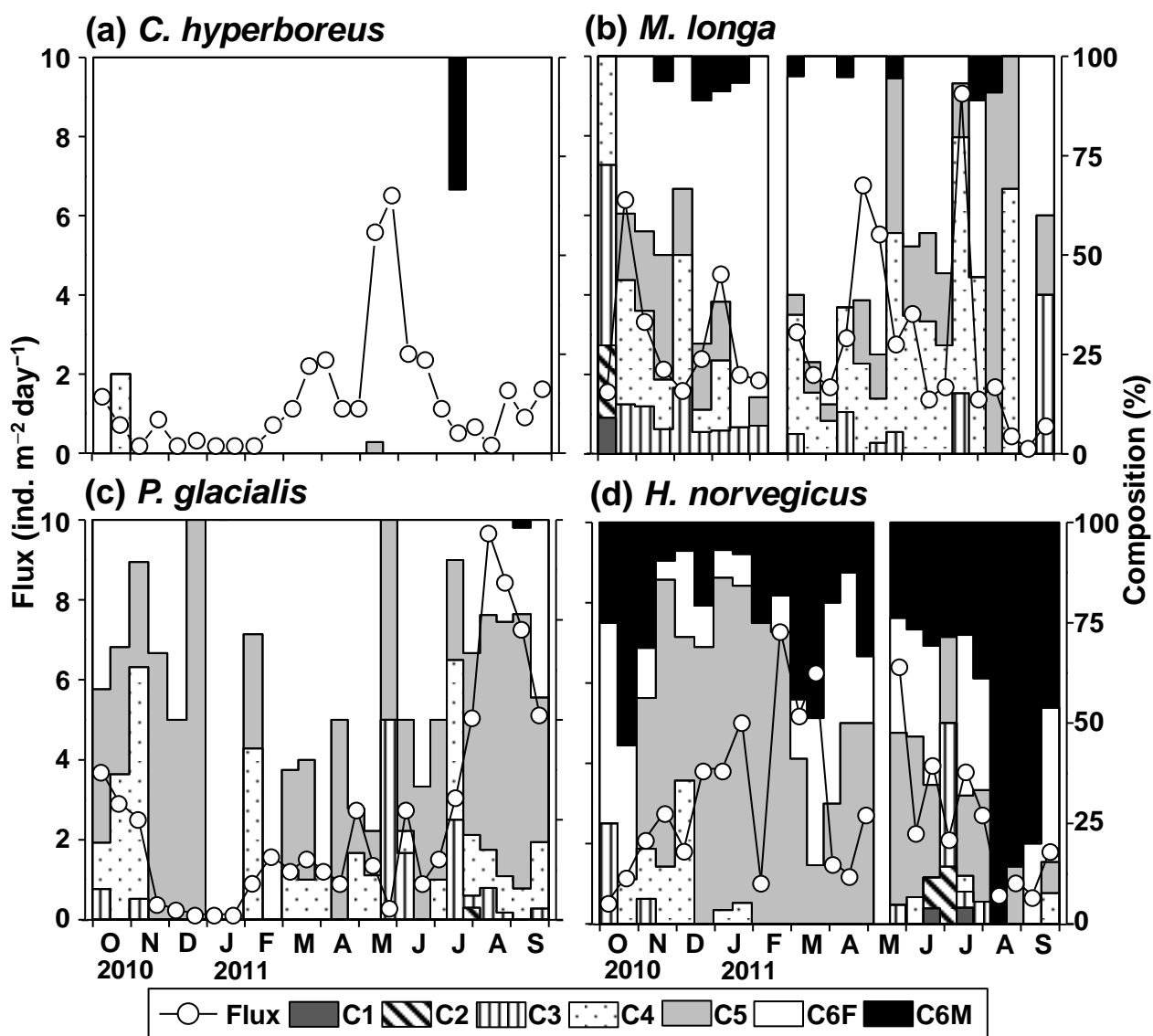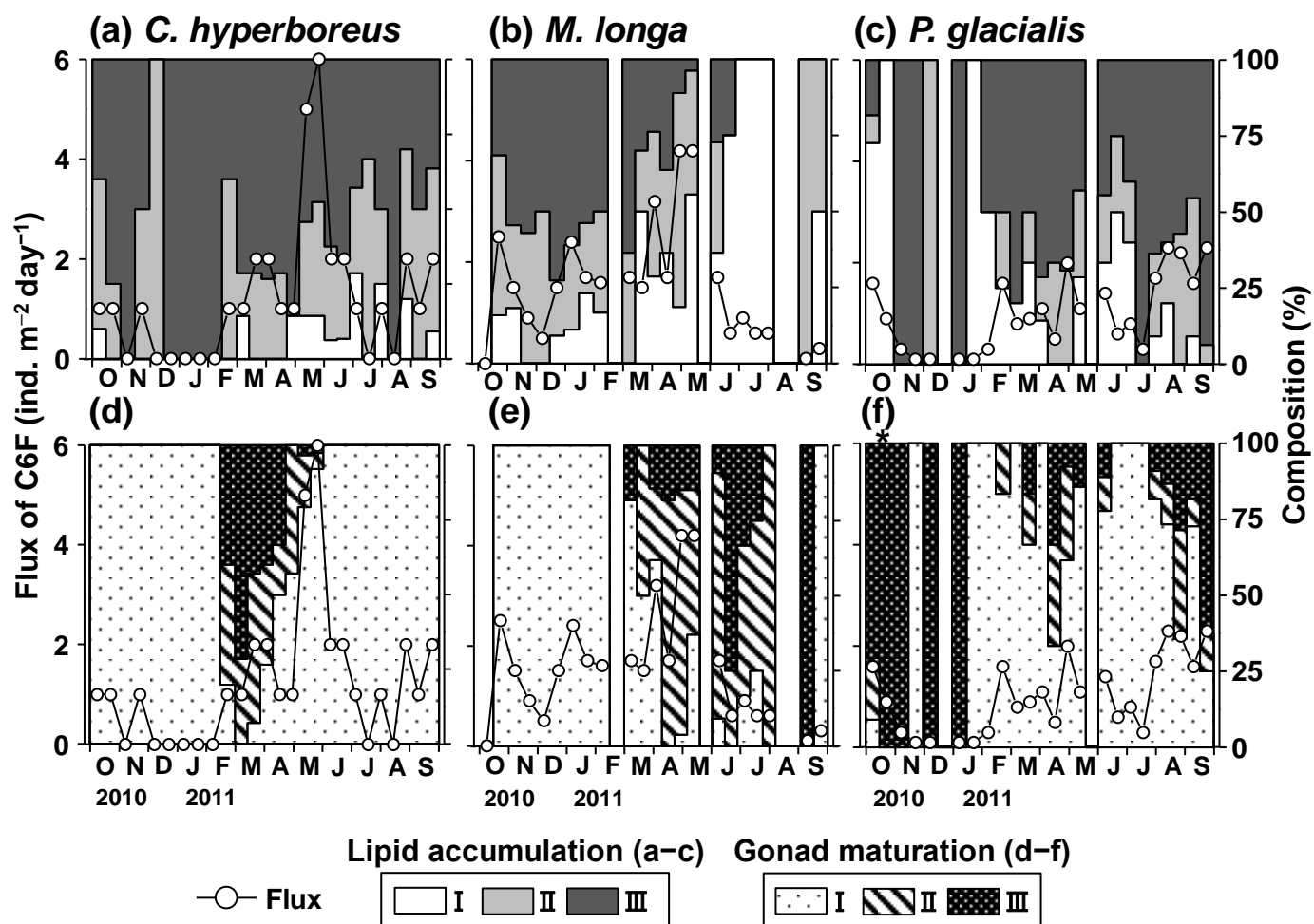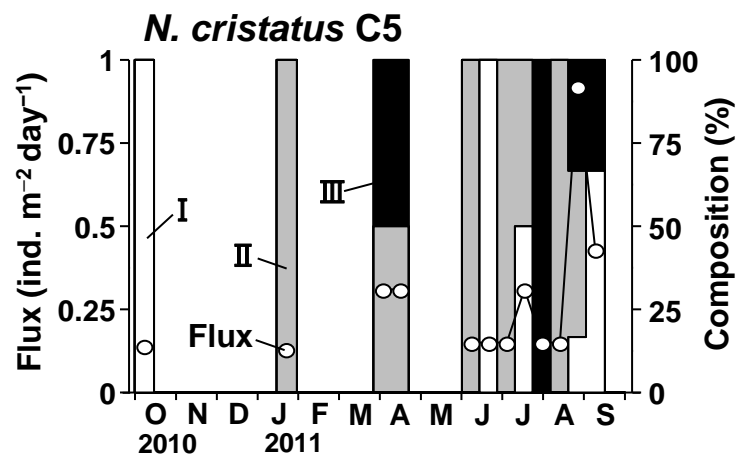
Fig. 5 (Matsuno et al.)

Fig. 6 (Matsuno et al.)

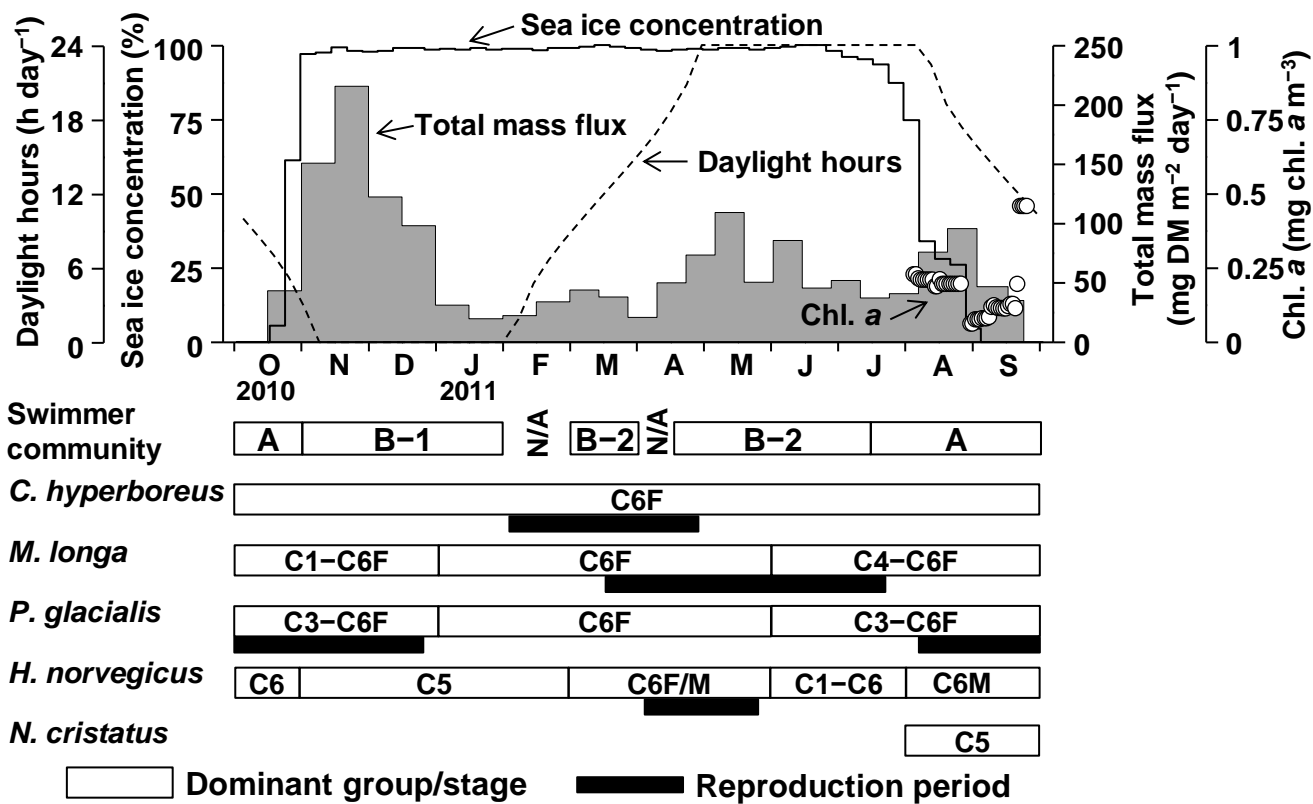Fig. 7 (Matsuno et al.)

Fig. 8 (Matsuno et al.)